Romanian Reports in Physics, Vol. 66, No. 4, P. 1099–1109, 2014

DECONVOLUTION OF THE LINE SPECTRA OF MICROSIZE LIGHT SOURCES IN MAGNETIC FIELD*

G. REVALDE[1,2], N. ZORINA[2], A. SKUDRA[2], Z. GAVARE[2]

[1] Riga Technical University, Institute of Technical Physics, Kalku str.1, LV 1050, Riga, Latvia, E-mail: Gita.Revalde@rtu.lv
[2] University of Latvia, Institute of Atomic Physics and Spectroscopy, Skunu 4, LV-1050,Riga, Latvia, E-mail: natalja.zorina@gmail.com; askudra@latnet.lv, Email: zanda.gavare@gmail.com

Received July 30, 2013

Abstract. We present our investigation of narrow spectral lines, emitted from microsize mercury/xenon electrodeless light source in magnetic field. The spectral line shapes were registered by the Fourier transform spectrometer and deconvoluted by means of a regularisation method. Two approaches were used to obtain the regularisation parameter. The plasma temperature and magnetic field intensity were obtained.

Key words: electrodeless light sources, microsize light sources, line shapes, Zeeman Effect, inverse problem, Tikhonov's regularisation method, calculated real line shape, low-pressure plasma temperature, regularisation parameter, instrumental function of the Fourier transform spectrometer.

1. INTRODUCTION

Our research is devoted to the preparation and optimisation of special type of electrodeless light sources for their use in different scientific devices [1]. Such light sources can be used in atomic absorption devices or as standards. Due to recent trends of miniaturisation, there is a need to find out right methods of diagnostics for small scale plasmas. In this paper we show our experience of diagnostics of micrometer size capillary lamps by means of spectral line shape measurements with Fourier transform spectrometer (FTS). Since the capillary sources emit very narrow lines, it is a challenge to get information about the form of spectral lines, though it is important for application of the lamps in high precision experiments.

In our previous research we did experiments of line shape investigation with such devices as Fabry Perrot spectrometer [2] and Zeeman scanning spectrometer [3, 4]. However, these methods have several restrictions and are not applicable for microsize light source diagnostics. FTS are becoming more and more widely used

* Paper presented at the 16th International Conference on Plasma Physics and Applications, June 20–25, 2013, Magurele, Bucharest, Romania.

in different experiments, where very high precision, especially in the IR spectral range, is needed. Though the light sources under investigation are used mainly in UV and visible spectral region, FTS can be used in this case too. The broadening of lines emitted from the capillary lamps is on the same order as the instrument function of FTS.

In this work we present investigation of the influence of FTS instrument function on spectral line shapes, used for diagnostics of capillary light sources. The method of diagnostics consists of obtaining the measurements of line shapes and following retrieval of the calculated real line shape from experimental shapes by means of the Tikhonov's regularisation method. In [5, 6] we reported the first results for capillary light source filled with mercury and buffer gases. Different emission properties were observed depending on the working position of capillary. In [7] the method of imaging and tomography was used to investigate this phenomenon. Detailed investigation of the influence of approximation of the instrument function of FTS was done in this work. In addition, two methods for finding the regularisation parameter were applied.

2. EXPERIMENTAL

The capillary lamps under investigation were manufactured at the Institute of Atomic Physics and Spectroscopy in Riga. The length of the capillary was of 2 cm and the discharge size was of 500 μm in radius (Fig. 1a). A Fourier transform spectrometer is basically a Michelson interferometer. Beam splitter is used in this type of interferometer to divide an incoming light beam in two parts. The first part is reflected on a fixed mirror, whereas the second part is reflected on a mobile mirror. The two beams are recombined at the beam splitter and shone on a detector. The principal scheme is shown below (Fig. 1b).

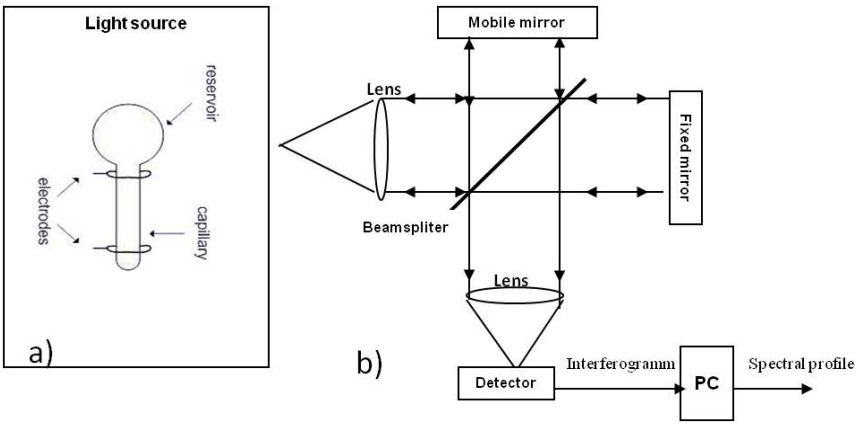

Fig. 1 – a) Design of the capillary electrodeless light source; b) Scheme of Fourier transform spectrometer as a Michelson interferometer.

At the end of capillary the lamp contains small reservoir for metal vapour. The discharge is ignited in the capillary part of lamp. In this case the lamp was filled with xenon of 2 Torr partial pressure and mercury isotope 198. The reservoir at the end of lamp is used as a cold spot to control the metal vapour pressure in lamp [8]. In this experiment the mercury isotope pressure was of 0.003 Torr [9].
The lamps were capacitatively excited using 100 MHz frequency applied to external electrodes. The lamps were operated in three different positions in accordance to the Earth plane, namely, horizontally, vertically with Hg reservoir up, and vertically with Hg reservoir down. The lamps were placed in magnetic field to observe Zeeman splitting, as necessary for their application in Zeeman Atomic Absorption Spectrometry (ZAAS). Magnetic field was perpendicular to the axis of capillary and the direction of observation was parallel to the magnetic field lines.

Spectral lines, emitted from Hg/Xe high frequency microsize capillary lamp, were measured using Fourier Transform spectrometer *Bruker IFS-125HR,* capable of registering lines in the wavelength region 330–2000 nm. We analyse the 404.7 nm Hg spectral line in this paper in detail. The examples of experimental measurements of the 404.7 nm line in three different working positions are shown in Fig. 2. As clearly can be seen in Fig. 2, the most intensive lines were obtained when the lamp was operated vertically, especially with the reservoir up. The smallest intensity was observed when the lamp was operated horizontally. This effect was observed in our previous research too, where we found that there is a difference between the distributions of atoms in different working positions [7].

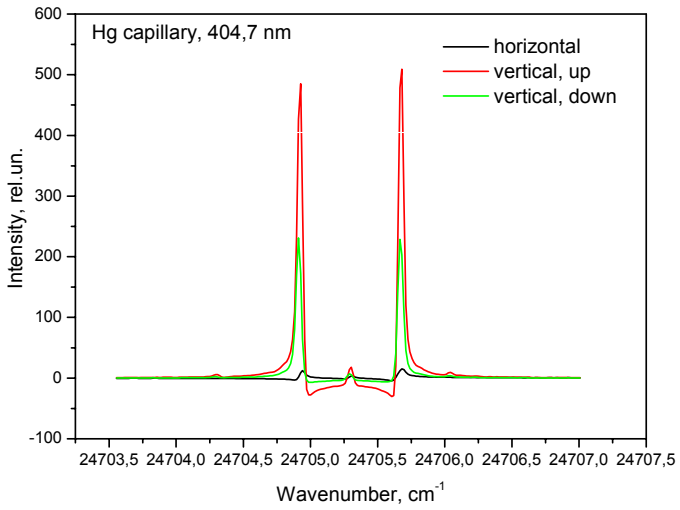

Fig. 2 – Example of experimentally measured Hg 404.7 nm line. The line was emitted from Hg/Xe capillary light source placed in three different working positions: horizontally (black line), vertically with Hg reservoir up (red line), and vertically with Hg reservoir down (green line).

3. THEORY

3.1. TIKHONOV'S REGULARISATION

For high precision spectroscopy it is necessary to retrieve the calculated real spectral line shape from the spectral line shape measured experimentally. The Fredholm first kind integral equation describes the convolution of real spectral line profile, measured (experimental) spectral line profile, and instrumental function:

$$\int_a^b A(x,s)y(s)\mathrm{d}s = f(x), \quad c \le x \le d, \tag{1}$$

where: *f(x)* – measured spectral line profile; *y(s)* – calculated real spectral line profile; *A(x,s)* – instrument function.

To retrieve the calculated real spectral line profile from experimental one without the instrumental function, it is necessary to solve the inverse ill-posed problem. Tikhonov's regularisation algorithm [10, 11] is one of the most useful tools for solving the task where small experimental uncertainties can cause large deviations in the solution.

Assuming, that the values on the right side and integral equation (1) kernel are known with accuracy:

$$\left.\begin{aligned} \left\| \tilde{f} - f \right\|_F &\le \delta; \\ \left\| \tilde{A} - A \right\| &\le \xi \end{aligned}\right\}, \tag{2}$$

where δ is the error of right part of (1) or the error of experimental $f(x)$ profile, ξ is the error of kernel of (1) or the error of instrument function $A(x,s)$, Tikhonov proved, that the initial, ill-posed task can be transformed into a task of searching for the minimum of smoothing functional:

$$M_\alpha\left[y, \tilde{f}\right] = \inf_{y \in Y} M_\alpha\left[y, \tilde{f}\right], \tag{3}$$

where: smoothing functional $M_\alpha\left[y, \tilde{f}\right]$, so called Tikhonov's functional, is given in the form:

$$M_\alpha\left[y, \tilde{f}\right] = \left\| \tilde{A}y - \tilde{f} \right\|_F^2 + \alpha\Omega[y], \tag{4}$$

stabilising functional Ω is described by the following expression:

$$\Omega[y] = \|y\|_Y^2, \tag{5}$$

where: $\alpha > 0$ – regularisation's parameter; number $\left\|\tilde{A}y - \tilde{f}\right\|_F^2$ discrepancy.

According to Tikhonov's method, instead of the initial ill posed problem, which is described by Fredholm integral equation of first kind, we get well posed task, which is described by Fredholm integral equation of second kind, which after changing the integrals to finite sums can be written as the system of linear equations:

$$\sum_{i=1}^{N} b_i \left(\sum_{m=1}^{N} b_m \tilde{A}_{mk} \tilde{A}_{mi} \right) y_i + \alpha y_k = \sum_{m=1}^{N} b_m \tilde{A}_{mk} \tilde{f}_m, \quad k = \overline{1, N} \tag{6}$$

or as matrix equation:

$$\left(\tilde{A}^* \tilde{A} + \alpha E\right) Y = \tilde{A}^* \tilde{f}, \tag{7}$$

where A_{ij} – elements of $N \times N$ size matrix A, which approximates kernel $K(x,x)$; f_i – vectors-column with initial dates; y_i – vector-column of solution; b_i – the coefficients of quadrature formula .

The mathematical model in detail is described in [4], in which Zeeman Scanning spectrometer was used for the registration of spectral lines.

3.2. REGULARISATION PARAMETER

It is well known, that the finding of regularisation parameter is crucial for application of Tikhonov's regularisation method. Two independent methods were used in this work to obtain the regularisation parameter α:

1) the minimisation of discrepancy [11]:

$$\left\|\tilde{A}y_\alpha - \tilde{f}\right\|_{L_2}^2 = \min_\alpha \left\|\tilde{A}y_\alpha - \tilde{f}\right\|_{L_2}^2; \tag{8}$$

2) the Kojdecki method [12]. According this method α is root of equation:

$$\alpha^{q+1} \left\| y_\alpha \right\| = \beta \, \| \tilde{A} \| \left(\delta + \xi \left\| y_\alpha \right\| \right). \tag{9}$$

In this work α was obtained from (9) in supposition that the error of kernel $\xi = 0$. The coefficients were chosen as $q = 0$ and $\beta = 1$. Variance of the errors of measured line is 0.017.

3.3. INSTRUMENT FUNCTION FOR FOURIER TRANSFORM SPECTROMETER

To obtain the calculated real profile from measured spectral profile by means of regularisation, it is necessary to know the instrument function very accurately.

First, we used an experimentally measured He spectral line of 632.8 nm wavelength emitted from the single mode He/Ne laser as a data array for instrument function matrix A in the formula (7) for deconvolution without any approximation, but it led to false maximums, especially in the far wings of the profile.

Second step was to test the instrument function given by the theory of Fourier transform spectrometry [13, 14], causing restrictions of the resolution of the device due to the limited optical path difference in the Michelson interferometer inside the Fourier transform spectrometer:

$$I(x) = 2L \bmod \left\{ \operatorname{sinc}\left[2\pi (x_0 - x) L \right] \right\} \tag{10}$$

where L – difference between lengths of two optical paths (optical path difference).

As we can see, usage of this function gives a lot of negative values and also false beats in the wings, where no real maxima can be present [14].

Afterwards we performed approximations of the instrument function trying to fit it with several known peak functions, for example, Voigt, Gauss and Lorentz functions.

The Voigt function was written in the form:

$$y = y_0 + A \frac{2\ln 2}{\pi^{3/2}} \frac{w_L}{w_G^2} \cdot \int_{-\infty}^{\infty} \frac{\mathrm{e}^{-t^2}}{\left(\sqrt{\ln 2}\, \dfrac{w_L}{w_G} \right)^2 + \left(\sqrt{4\ln 2}\, \dfrac{x - x_c}{w_G} - t \right)^2} \mathrm{d}t , \tag{11}$$

where w_L is full width at half of maximum (FWHM) of Lorentz function, w_G is FWHM of Gauss function, A – area, x_c – frequency at the line centre.

The Lorentz function was written in the form:

$$y = y_0 + 2Aw / \left(4\pi \left(x - x_c \right)^2 + w^2 \right), \tag{12}$$

where w – the FWHM of the line.

The Gauss function:

$$y = y_0 + \frac{A}{w\sqrt{\pi / 2}} \mathrm{e}^{-2\frac{(x - x_c)^2}{w^2}}, \tag{13}$$

where w – FWHM of the Gauss function.

Figure 3 shows the respective fitting results for the experimental instrument function (He laser line). We can see the experimental instrument function and its approximation with the Voigt function (fitting parameters are: the FWHM of Gaussian part ω_G is of 0.02926 (0.02012) cm^{-1}, the FWHM of the Lorentz part ω_L is of 0.02926 (0.01854) cm^{-1}); the fit to the Lorentz function (fitting parameters are: the FWHM ω_L is of 0.02862 (0.00341) cm^{-1}), and the fit to the Gauss function (fitting parameters are: the FWHM ω_G is of 0.03974 (0.00247) cm^{-1}).

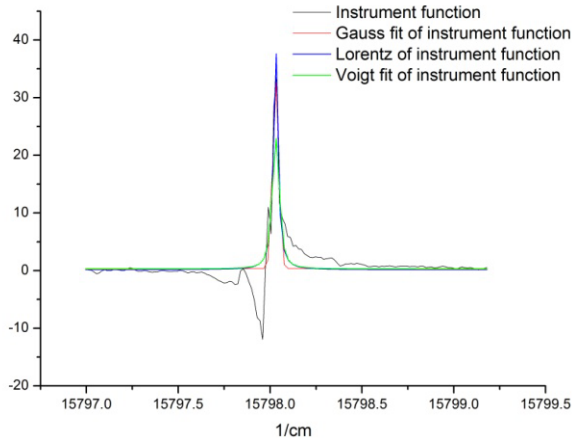

Fig. 3 – The experimentally measured instrument function (black line) of the Fourier transform spectrometer Bruker IFS-125HR and its approximation: the Voigt function (green line); the Lorentz function (blue line); the Gauss function (red line).

The best fitting results were obtained for the fitting with the Lorentz function (FWHM of 0.03 cm^{-1}), so we decided to use it for further tests.

In Fig. 4 the examples of deconvolution are shown when the instrument function was taken as a data array (blue line), Lorentz function (red line) and as a function described by Eq. 10 (green line). Figure 4 shows the deconvolution example for the measured 546 nm Hg line, emitted from Hg/Ar lamp without magnetic field. The example clearly demonstrates the case when the self-absorption dip in the centre of spectral line is covered by the instrument function.

The comparisons in figures below clearly demonstrate that the deconvolution procedure in cases, when instrument function was taken in a form of raw data, or as a theoretical instrument function described by equation (10), gave very noisy solutions on the wings of profiles. Also, this test illustrates that the best approximation of instrument function was its approximation with the Lorentz function.

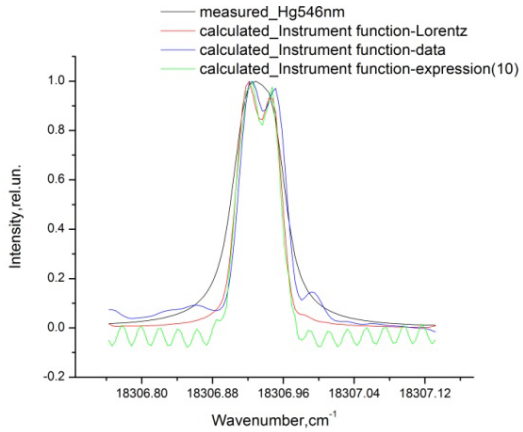

Fig. 4 – The example of the measured Hg 546 nm spectral line (black line) and calculated real lines in the case, when instrument function was taken as a data array (blue line), Lorentz function (red line) and as a function described by Eq.10 (green line). Line was emitted from Hg/Ar lamp without magnetic field.

4. RESULTS AND DISCUSSION

Figures 5a and 5b show the results for the vertical lamp operation, with Hg reservoir up and Hg reservoir down, respectively. All experimental lines were normalised for the line shape calculations and deconvolution. The line is split due to the Zeeman effect into one non-shifted π component and two σ components. The deconvolution was done using two independent methods Eq. (8) and Eq. (9) for finding the regularisation parameter.

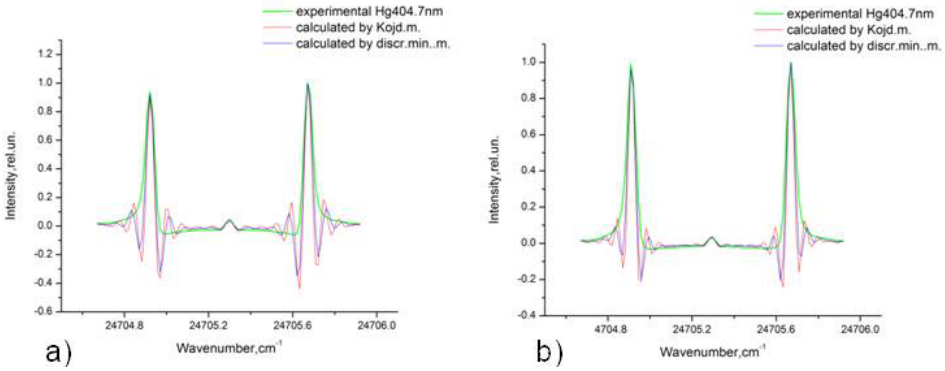

Fig. 5 – Measured and deconvoluted Hg 404.7 nm profiles: green line – experimental profile; blue and red lines – calculated real profiles, obtained using discrepancy minimization method for the getting of the regularisation parameter, and method when α is root of Eq. (9), respectively. a) Lamp was operated vertically with Hg reservoir up; b) lamp was operated vertically with Hg reservoir down**.**

After the deconvolution we performed Gauss fit to the calculated real lines, using expression (13).

In the Table 1 we can see the values of the full width at half of maximum (FWHM) of the Gauss profile. The values are shown for the Hg 404.7 nm emission line for vertical position of the lamp. The results of the solutions are shown for both methods of finding the regularisation parameter.

Table 1

The results of the deconvolution: the FWHM of the calculated real line shapes from the Gauss fit to the calculated real profiles for the Hg 404.7 nm emission line for both vertical positions of the lamp

FWHM(cm^{-1}) after Gauss fit	Peak 1	Peak 2	Peak 3	Lamp position
Experimental	0.05020	0.03148	0.04746	Vertically, with Hg reservoir up
Real calculated (discr.min.met.)	0.03541	0.03892	0.03437	
Real calculated (Kojdecki met.)	0.02893	0.02901	0.02826	
Experimental	0.05072	0.03176	0.05036	Vertically, with Hg reservoir down
Real calculated (discr.min.met.)	0.03518	0.02720	0.03539	
Real calculated (Kojdecki met.)	0.02873	0.02946	0.02903	

Both methods give credible results. However, we can observe that the Kojdecki method gives smaller values of the FWHM of the calculated real line shape than discrepancy method. It can be explained by the fact that the method proposed by Kojdecki strongly depends on errors of measurements and instrumental function. For application of the discrepancy minimization method it is necessary to know only the instrument function. We can also observe that the signal for the horizontal lamp position is very weak (see Fig. 2); therefore, the results of calculations for this working position were not taken into account for temperature estimation.

The motion of atoms in accordance to the Maxwell law is isotropic in the space, and therefore the width at half of maximum (FWHM) corresponds to the Doppler effect. Thus, the temperature of radiating atoms can be obtained by the following expression [15, 16]:

$$T = \frac{\mu}{\left(7.16 \times 10^{-7} x_0\right)^2} \Delta x_D^2 \,, \tag{14}$$

where T is the absolute temperature of emitting atoms, μ – the atomic mass, x_0 – the position of the scale of the frequencies, when the Gauss function reaches its maximum value, and Δx_D – the FWHM of Gaussian function. The average

calculated temperature value of radiating atoms is of 653.5 K, which is in good agreement with our initial calculations [5]. The relative error is 19%. No clear evidence of the temperature changes in different working positions was found. In addition, the magnetic field intensity was calculated from the Zeeman splitting of the spectral lines. The separation of the components Δx is dependent on the intensity of magnetic field $\boldsymbol{H}$:

$$\Delta x = \frac{1}{4\pi c}\frac{e}{m}\boldsymbol{H}. \tag{15}$$

Here e and m stands for charge and mass of electron, c – speed of light. Using this formula, we get the value of 4016 oersted ($3.1958 \cdot 10^5$ A/m) for the intensity of magnetic field. Further investigations are necessary to estimate the role of magnetic field inhomogeneity on the broadening of the line shapes.

5. CONCLUSION

In this paper we report the investigation of narrow multiple line shapes by means of the Fourier transform spectrometer. The lines were emitted from microsize capillary Hg/Xe discharge lamps, placed in magnetic field. Line shapes were deconvoluted from instrument function by means of the Tikhonov's regularisation method. Detailed analysis of the instrument function of the Fourier transform spectrometer was performed, leading to the conclusion that the best approximation for regularisation method was approximation with the Lorentz function. We proved the possibility to obtain the regularisation parameter by two different ways; however, more statistical data are necessary for the usage of Kojdecki method. The calculated temperature value of radiating atoms is of 655 K, which is in good agreement with our initial calculations [5]. Further research is necessary to understand the influence of operation position and magnetic field on the processes in the capillary discharge plasma.

Acknowledgments. G.Revalde acknowledges the support from the European Social Fund within the Project "Elaboration of Innovative Functional Materials and Nanomaterials for Application in Environment Control Technologies" 1DP/1.1.1.2.0/13/APIA/VIAA/30.

A.Skudra and Z.Gavare acknowledge the partial support from the ERDF project No.2010/0260/2DP/2.1.1.1.0/10/APIA/VIAA/166.

REFERENCES

1. A. Ganeev, Z. Gavare, V.I. Khutorshikov, S.V. Khutorshikov, G. Revalde, A. Skudra, G.M. Smirnova, N.R. Stankov, Spectrochimica Acta Part B, **58**, 879–889 (2003).
2. N. Zorina, Nuclear Instruments and Methods in Physics Research Section A, **623**, 763–765 (2010).
3. G. Revalde, A. Skudra, N. Zorina, S. Sholupov, J.Q.S.R.T., **107**,164–172 (2007).

4. N. Zorina, G. Revalde, R. Disch, in SPIE Sixth International Conference on Advanced Optical Materials and Devices, University of Latvia, Riga, **7142**, 71420J-1 (2008).
5. G. Revalde, N. Zorina, J.Skudra , A. Skudra, ICLS 2012, St. Petersburg, 2012.
6. G.Revalde, N.Zorina, A.Skudra, Imaging and Applied Optics: OSA Optics & Photonics Congress, 23–27 June 2013, VA, USA, JTu4A.12 (2013).
7. N. Denisova, G. Revalde, A. Skudra, and Ja. Skudra, Spatial Diagnostics of Hg/Ar and Hg/Xe Discharge Lamps by Means of Tomography, Jpn. J. Appl. Phys., **50**, 08JB03 (2011).
8. W. Bell, A.L. Bloom, Electrodeless discharge method and apparatus, US Patent 2975330, 1961.
9. *** Tables of physical quantities, Handbook, Moscow, Atomizdat, 199 (1976).
10. A. Tikhonov, V.Arsenin, *The solution's methods of the ill-posed problem*, Moscow, Nauka, 1979.
11. F. Verlan, V.S. Sizikov, *The integral equations: the methods, algorithms, program*, Kiev, Naukova Dumka, 1986.
12. M.A. Kojdecki, *New criterion of regularization parameter choice in Tikhonov's method*, Biuletyn WAT (Biul. Mil. Univ. Technol.), **49**, *1*, (569), 47–126 (2000).
13. V. Revalds, Spektrālie aparāti, University of Latvia, Part 3 (in Latvian), 1977, pp. 91–93.
14. P. Griffiths and J. de Haseth (Edit.), *Fourier transform infrared spectrometry*, Wiley & Sons, 1986.
15. E. Frish, Spectroscopy of the gas discharge plasma, Nauka, Leningrad, 25–26, 1970, p. 9.
16. W. Demtroeder, *Laser Spectroscopy*, third ed., Springer, 2003, p. 70.